JID Open

Acute Inhibition of MEK Suppresses Congenital Melanocytic Nevus Syndrome in a Murine Model Driven by Activated NRAS and Wnt Signaling

Jeffrey S. Pawlikowski[1,2,11], Claire Brock[1,2], Sheau-Chiann Chen[3], Lara Al-Olabi[4], Colin Nixon[2], Fiona McGregor[2], Simon Paine[4], Estelle Chanudet[5], Wendy Lambie[2], William M. Holmes[6], James M. Mullin[6], Ann Richmond[7,8], Hong Wu[9], Karen Blyth[2], Ayala King[1], Veronica A. Kinsler[4,10] and Peter D. Adams[1,2]

Congenital melanocytic nevus (CMN) syndrome is the association of pigmented melanocytic nevi with extra-cutaneous features, classically melanotic cells within the central nervous system, most frequently caused by a mutation of *NRAS* codon 61. This condition is currently untreatable and carries a significant risk of melanoma within the skin, brain, or leptomeninges. We have previously proposed a key role for Wnt signaling in the formation of melanocytic nevi, suggesting that activated Wnt signaling may be synergistic with activated NRAS in the pathogenesis of CMN syndrome. Some familial pre-disposition suggests a germ-line contribution to CMN syndrome, as does variability of neurological phenotypes in individuals with similar cutaneous phenotypes. Accordingly, we performed exome sequencing of germ-line DNA from patients with CMN to reveal rare or undescribed Wnt-signaling alterations. A murine model harboring activated $NRAS^{Q61K}$ and Wnt signaling in melanocytes exhibited striking features of CMN syndrome, in particular neurological involvement. In the first model of treatment for this condition, these congenital, and previously assumed permanent, features were profoundly suppressed by acute post-natal treatment with a MEK inhibitor. These data suggest that activated NRAS and aberrant Wnt signaling conspire to drive CMN syndrome. Post-natal MEK inhibition is a potential candidate therapy for patients with this debilitating condition.

Journal of Investigative Dermatology (2015) **135,** 2093–2101; doi:10.1038/jid.2015.114; published online 14 May 2015

INTRODUCTION

Congenital melanocytic nevus (CMN) syndrome (formerly known as neurocutaneous melanosis) is the involvement of typically large pigmented melanocytic nevi with extra-cutaneous features, such as certain facial characteristics and melanotic cells within the central nervous system (CNS; Barkovich *et al.*, 1994; Kinsler *et al.*, 2008; Kinsler *et al.*, 2012). Pigmented hairy nevi can cover up to 80% of the body surface area, and neurological abnormalities can lead to intractable seizures and neurodevelopmental delay. There is also a significant risk of primary melanoma within the skin, brain, or leptomeninges (Krengel *et al.*, 2006; Kinsler *et al.*, 2009). Previous work has shown that CMN syndrome is caused, in roughly 80% of cases, by a single post-zygotic mutation of *NRAS* codon 61 in a neuro-ectodermal precursor (Kinsler *et al.*, 2013b). However, some familial pre-disposition also suggests a germ-line contribution to the development of CMN (Danarti *et al.*, 2003; Kinsler *et al.*, 2009; de Wijn *et al.*, 2010). There is currently no treatment for this condition, and where melanoma develops the outcome is almost universally fatal. Despite recent advances in treatment of some types of melanoma with targeted therapies, a cure for melanoma harboring *NRAS* mutation remains particularly elusive (Shtivelman *et al.*, 2014). Therefore, a potential treatment for the cutaneous and extra-cutaneous features of CMN syndrome is most likely prior to its acquisition of additional genetic alterations *en route* to melanoma.

In both CMN and acquired melanocytic nevi, nevus cells are thought to be maintained in a proliferation arrested state

[1]*Institute of Cancer Sciences, University of Glasgow, Glasgow, UK;* [2]*Beatson Institute for Cancer Research, Glasgow, UK;* [3]*Center for Quantitative Sciences, Vanderbilt University Medical Center, Nashville, Tennessee, USA;* [4]*Genetics and Genomic Medicine, UCL Institute of Child Health, London, UK;* [5]*GOSgene, UCL Institute of Child Health, London, UK;* [6]*Institute of Neuroscience and Psychology, University of Glasgow, Glasgow, UK;* [7]*Department of Veterans Affairs, Vanderbilt University Medical Center, Tennessee Valley Healthcare System, Nashville, Tennessee, USA;* [8]*Department of Cancer Biology, Vanderbilt University Medical Center, Nashville, Tennessee, USA;* [9]*Fox Chase Cancer Center, Philadelphia, Pennsylvania, USA and* [10]*Pediatric Dermatology, Great Ormond St Hospital, London, UK*

Correspondence: Veronica A. Kinsler, Genetics and Genomic Medicine, UCL Institute of Child Health, London, UK or Peter D. Adams, Institute of Cancer Sciences, University of Glasgow, Glasgow,, UK. E-mail: v.kinsler@ucl.ac.uk or p.adams@beatson.gla.ac.uk

[11]*Current address: Department of Cancer Biology, Vanderbilt University Medical Center, Nashville, Tennessee, USA.*

Abbreviations: CMN, congenital melanocytic nevus; CNS, central nervous system

Received 12 January 2015; revised 2 March 2015; accepted 9 March 2015; accepted article preview online 27 March 2015; published online 14 May 2015

by cellular senescence (Michaloglou *et al.*, 2005; Gray-Schopfer *et al.*, 2006; Suram *et al.*, 2012), a tumor-suppressive, stable proliferation arrest triggered by activated oncogenes and other molecular stresses (Salama *et al.*, 2014). A complex network of effectors enacts the senescence response, including DNA damage signaling, activation of the pRB and p53 pathways and, notably, repression of Wnt signaling (Ye *et al.*, 2007; Pawlikowski *et al.*, 2013; Juan *et al.*, 2014; Salama *et al.*, 2014). Paradoxically, however, we and others have shown that nevus melanocytes, including in CMN, often exhibit markers of activated Wnt signaling (Bergman *et al.*, 1997; King *et al.*, 2001; Ramirez *et al.*, 2005; Kinsler *et al.*, 2013a; Pawlikowski *et al.*, 2013), and activated Wnt signaling is able to bypass or delay senescence in mouse models (Delmas *et al.*, 2007; Pawlikowski *et al.*, 2013; Juan *et al.*, 2014). We therefore reasoned that activated Wnt signaling, in addition to the *NRAS* mutation, might influence the varied phenotype of CMN syndrome.

RESULTS

Altered Wnt signaling in human CMN syndrome

To more directly assess the status of Wnt signaling in human CMN, we stained such nevi for markers of activated Wnt signaling. As shown previously (Kinsler *et al.*, 2013a), CMN expressed nuclear and cytoplasmic localized β-catenin. In addition, these nevi consistently expressed cyclin D1 and c-MYC (Figure 1) indicative of activated Wnt signaling and in contrast to normal epidermal melanocytes that do not express nuclear cyclin D1 and c-myc (Pawlikowski *et al.*, 2013). We conclude that human CMN are associated with activated Wnt signaling.

A higher prevalence of CMN within some families suggests a germ-line predisposition to CMN (Danarti *et al.*, 2003; Kinsler *et al.*, 2009; de Wijn *et al.*, 2010), and neurological phenotypic variability between patients with similar cutaneous phenotypes also supports a role for a modifying germline genotype. Accordingly, we performed whole-exome next-generation sequencing on DNA from peripheral white blood cells of 32 children with extensive CMN (phenotypic classification in Supplementary Table S1 online). In CMN syndrome, mutation of *NRAS* is a somatic event (Kinsler *et al.* 2013b). Therefore, in these blood samples, *NRAS* is wild type in all cases. Using the filters described in the Supplementary Materials and Methods online to identify rare variants in Wnt signaling pathway genes, 3,213,226 calls were reduced to 32 variants in 26 genes that occur with a prevalence $<0.5\%$ in control population databases and to 34 variants in 26 genes at $<1\%$ prevalence. After manually reviewing the BAM files, 20 variants in 32 patients were judged sufficiently convincing on all parameters to investigate further, and of these 19 were confirmed by Sanger sequencing. One was not confirmed, and one was not able to be confirmed because of lack of patient sample but was sufficiently convincing on next-generation sequencing to be included in the analyses. Genetic variation in *FZD1* was seen in six CMN patients and therefore considered a possible undescribed SNP (pending confirmation of its prevalence by direct screening of a large control population). These 19 variants seen in 14 CMN patients are listed in Table 1. This list includes variants in the *APC, APC2*, *FZD6*, *TCF3*, and *WNT16* genes that are absent from control population databases. Although functional characterization of each individual variant is beyond the scope of the current study, this analysis is supportive for a role for germ-line alterations of Wnt signaling, together with somatic activation of NRAS, in the development of extensive CMN.

Activation of Wnt signaling and NRAS recapitulates CMN syndrome in a mouse model

On the basis of this finding, we asked whether combined activation of NRAS and Wnt signaling in the melanocytic lineage could drive formation of CMN syndrome in an animal model. We therefore generated mice with either activated NRAS (*Tyr-NRas^{Q61K}* (Ackermann *et al.*, 2005) or activated Wnt signaling alone (*Tyr-Cre Apc$^{fl.fl}$* (Shibata *et al.*, 1997)) or both activated NRAS and Wnt signaling (*Tyr-Cre Apc$^{fl.fl}$/Tyr-NRas^{Q61K}* (Pawlikowski *et al.*, 2013)), all under the control of the mouse *Tyr* promoter to restrict altered signaling largely to the melanocytic lineage (Delmas *et al.*, 2003). These mice were then examined for features characteristic of CMN syndrome in humans, including skin hyperpigmentation and excessive infiltration of pigmented melanocytes into the leptomeninges and brain (Supplementary Figure S1 online). As reported previously, *Tyr-NRas^{Q61K}* mice

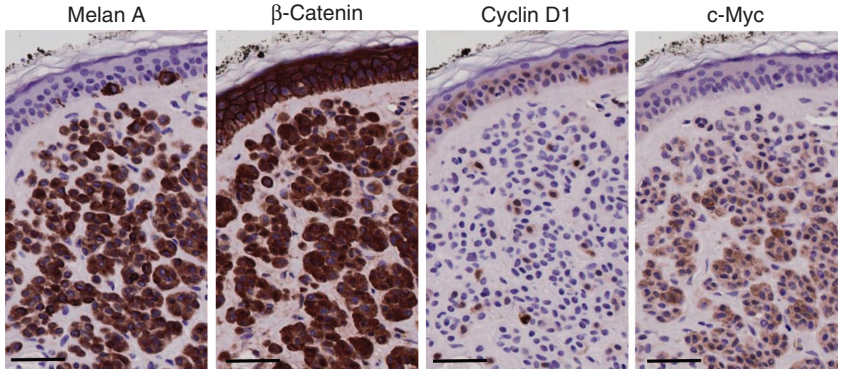

Figure 1. Human congenital melanocytic nevi harbor activated Wnt signaling. Serial sections of a CMN stained for melan A, β-catenin, cyclin D1, and c-myc. Images are representative of at least four congenital human nevi (Scale bar = 25 μm).

Table 1. Details of 19 rare germline variants found in 14 CMN patients on whole-exome sequencing

Gene symbol	Position (Hg19)	Reference allele/Sample allele	Protein variants	Translation impact	Predicted functional impact: SIFT function prediction (score), PolyPhen-2 function prediction	Conservation phyloP p-value (http://compgen.bscb.cornell.edu/phast/help-pages/phyloP.txt)	dbSNP ID (http://www.ncbi.nlm.nih.gov/SNP/)	Frequency in control population: 1,000 Genomes/CG public genomes/NHLBI ESP
APC	5:112176056	C/T	p.R1571C; p.R1589C	Missense	Damaging (0.05, possibly damaging	0.005152		—/—/0
APC2	19:1453017	C/T	p.A6V	Missense	Damaging (0.05), probably damaging	1.83E–05	rs200897976	0.19/—/0.02
APC2	19:1465820	5′-GGCCAA GGCCAAGGCC AAG-3′/5′-GGCC AAGGCCAAGGCC AAGGCCAAG-3′	p.K846_L847insAK	In-frame				—/—/0
EP300	22:41569633	A/G	p.K1542E	Missense	—, Possibly damaging	3.52E–04	rs374162524	—/—/0.01
FZD1	7:90894459	ACC/ACCACC	p.P89_P90insP	In-frame				—/—/0
FZD6	8:104341919	AT/—	p.C527*; p.C495*	Frameshift				—/—/0
HNF1A	12:121426790	G/A	p.A161T	Missense	Damaging (0.03), probably damaging	1.32E–04	rs201095611	—/—/0.01
LRP1	12:57577915	C/T	p.R1993W	Missense	Damaging (0), probably damaging		rs141826184	0.05/—/0.22
LRP1	12:57602881	A/T	p.Y4054F	Missense	Damaging (0.02), probably damaging	2.47E–05	rs79435985	0.96/—/0
MAP4K1	19:39108034	G/A	p.R70W	Missense	Damaging (0), probably damaging		rs35079766	0.11/—/0.11
PPP2R1B	11:111608216	T/A	p.N623Y; p.N559Y	Missense	Damaging (0.01), possibly damaging		rs61756429	0.35/0.92/0.76
PPP2R1B	11:111631738	AC/—	p.V115fs*3; p.V51fs*3	Frameshift		2.11E–05		—/—/0.06
PPP2R3B	X:308383	C/T	p.A186T	Missense	Damaging (0.04), possibly damaging	7.33E–05		—/—/0.05
RARB	3:25636151	C/T	p.R266C; p.R378C	Missense	Damaging (0), probably damaging	1.03E–06		—/—/0
SOX8	16:1034833	A/T	p.N263I	Missense	Damaging (0.01), possibly damaging	1.88E–03	rs201359112	—/—/0
TCF3	19:1621908	GAGGAG/GAG	p.S295del	In-frame		1.07E–03		—/—/0
TCF7	5:133480486	A/G				1.31E–05	rs201733691	—/—/0.04
WNT16	7:120965470	—/CCA	p.M1fs*141	Frameshift				—/—/0
WNT9B	17:44950095	G/A	p.R97H	Missense	Damaging (0), probably damaging	1.93E–06	rs201223229	0.06/—/0

Abbreviation: APC, adenomatous polyposis coli.
Whole-exome sequencing was performed on peripheral blood leukocyte DNA from children with CMN. Data were analyzed to identify rare pathogenic variants (<1% of the population in published control data sets) in genes in the APC/Wnt-signaling pathway.

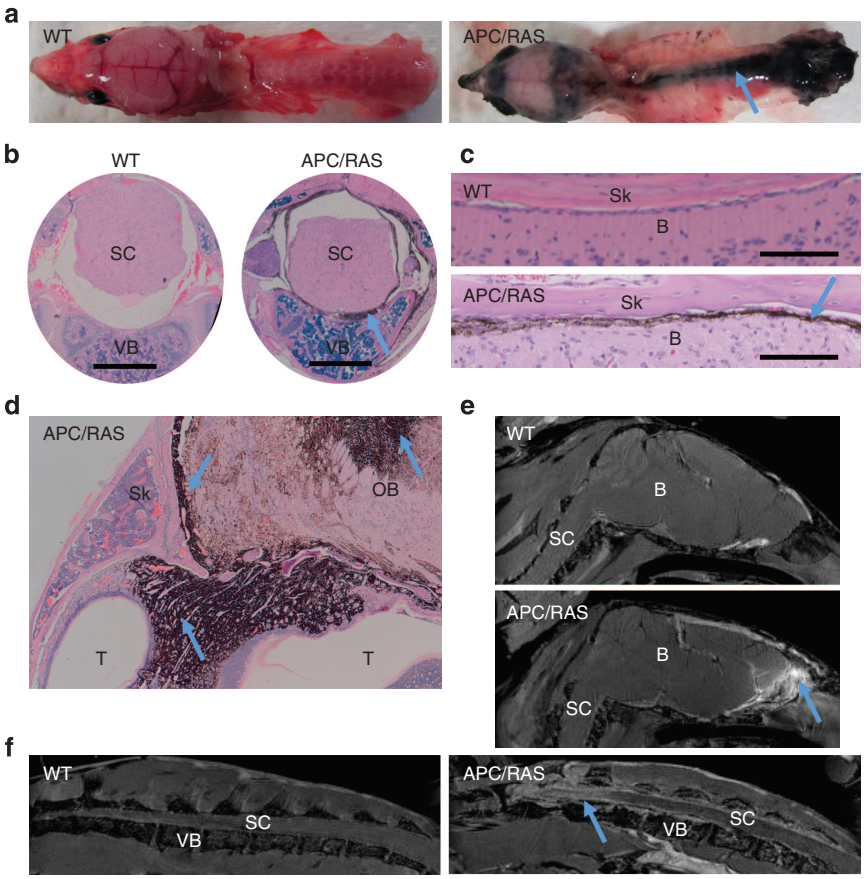

Figure 2. A mouse model harboring activated RAS and Wnt signaling recapitulates human CMN syndrome. (**a**) Representative images of blackened spine and head in 2-week-old *Tyr-Cre* $Apc^{fl.fl}$/*Tyr-*$NRas^{Q61K}$ mice (right (representative of >60 mice)) compared with wild-type mice (left). *Tyr-Cre* $Apc^{fl.fl}$ and *Tyr-*$NRas^{Q61K}$ were indistinguishable from wild-type mice in these respects (not shown). (**b**) Transverse H+E section showing melanocytic infiltration (melanin) into leptomeninges of the spine of *Tyr-Cre* $Apc^{fl.fl}$/*Tyr-*$NRas^{Q61K}$ mouse (right) compared with wild-type mouse (left). (**c**) Longitudinal H+E section showing melanocytic infiltration (melanin) into leptomeninges of the brain of *Tyr-Cre* $Apc^{fl.fl}$/*Tyr-*$NRas^{Q61K}$ mouse (bottom) compared with wild-type mouse (top). (**d**) Melanocytic infiltration of cartilage and the olfactory system of *Tyr-Cre* $Apc^{fl.fl}$/*Tyr-*$NRas^{Q61K}$ mouse. (**e**) Longitudinal MRI showing melanocytic invasion (white) into the head in *Tyr-Cre* $Apc^{fl.fl}$/*Tyr-*$NRas^{Q61K}$ mouse (bottom) compared with wild-type mouse (top). (**f**) Longitudinal MRI showing melanocytic invasion (white) around spine in *Tyr-Cre* $Apc^{fl.fl}$/*Tyr-*$NRas^{Q61K}$ mouse (right) compared with wild-type mouse (left). Blue arrows indicate melanocytic infiltration. APC, adenomatous polyposis coli; B, Brain; CMN, congenital melanocytic nevus; MRI, magnetic resonance imaging; OB, Olfactory Bulb; SC, spinal cord; Sk, Skull; T, Turbinates; VB, vertebral body; WT, wild type.

exhibited an excess of melanocytes in the dermis and became hyperpigmented with melanin within a few days of birth, compared with either wild-type mice or *Tyr-Cre* $Apc^{fl.fl}$ mice (Ackermann *et al.*, 2005; Pawlikowski *et al.*, 2013). Strikingly, activation of Wnt-signaling in *Tyr-Cre* $Apc^{fl.fl}$/*Tyr-*$NRas^{Q61K}$ mice greatly exacerbated the $NRas^{Q61K}$-induced proliferative expansion of melanocytes and skin melanization ((Supplementary Figure S2 online) and previously quantitated in (Pawlikowski *et al.*, 2013)), comparable to the cutaneous features of extensive CMN (Supplementary Figure S1A online). In addition, on post mortem, *Tyr-Cre* $Apc^{fl.fl}$/*Tyr-*$NRas^{Q61K}$ mice, but neither *Tyr-Cre* $Apc^{fl.fl}$ nor *Tyr-*$NRas^{Q61K}$ mice, were found to have neurological features characteristic of human CMN syndrome, including hyperpigmented spines (Figure 2a and Supplementary Figure S1B online) and the pathognomonic leptomeningeal melanosis around the spinal cord (Figure 2b and c). In the head, the mice showed melanosis and thickening of the leptomeninges, as well as melanosis in olfactory bulbs and nasal turbinates (Figure 2d). Invasion of melanin-producing cells around the spinal cord and into the brain was also observed by MRI (Figure 2e and f and Supplementary Figure S1C, S1D and Supplementary Video S1 online), highly reminiscent of the malignant progression seen in patients with CMN complicated by melanoma (Rhodes *et al.*, 1991; Kinsler *et al.*, 2008). The abnormal infiltrating pigment-producing cells in the mice were confirmed as melanocytes based on morphology, as well as expression of the neural crest cell marker S100 (Supplementary Figure S3 online).

Features of CMN syndrome are blocked through post-natal MEK inhibition

As proliferative expansion of the melanocyte population in the *Tyr-Cre* $Apc^{fl.fl}$/*Tyr-*$NRas^{Q61K}$ mice was dependent on

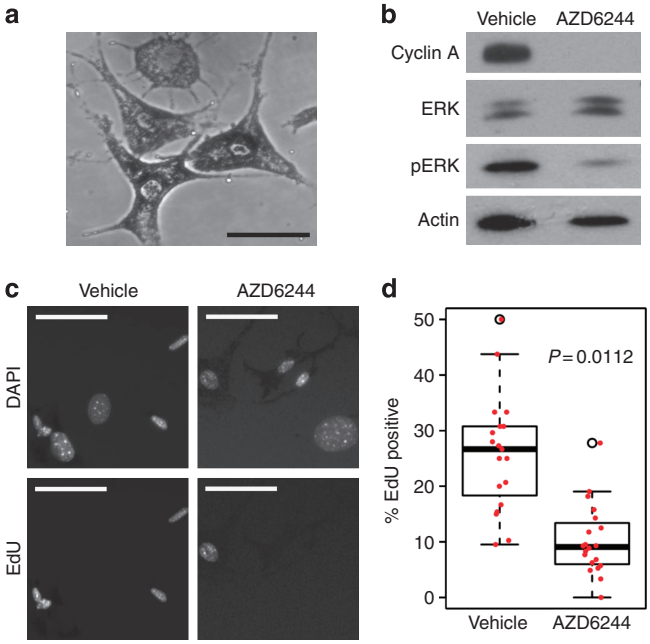

Figure 3. *Tyr-Cre Apc$^{fl.fl}$/Tyr-NRas^{Q61K}* mouse melanocytes are sensitive to MEK inhibition *in vitro*. (**a**) Phase contrast image of dendritic, pigmented melanocytes isolated from the skin of *Tyr-Cre Apc$^{fl.fl}$/Tyr-NRas^{Q61K}* mouse (Scale bar = 25 μm). (**b**) MEK inhibitor, AZD6244, downregulates phosphoERK and cyclin A expression. Cells were treated with DMSO vehicle or AZD6244, as indicated. (**c**) EdU labeling and DAPI stain of nuclei from **b** (Scale bar = 25 μm). (**d**) Quantitation of EdU labeling from (**c**). Results from three experiments, each scoring >100 DAPI-stained nuclei. Linear mixed-effects model was performed to compare the difference in percent EdU positive.

dual activation of NRAS and Wnt signaling, we reasoned that inhibition of NRAS signaling alone should be sufficient to inhibit proliferation of these cells. To test this *in vitro*, we prepared cutaneous melanocytes from *Tyr-Cre Apc$^{fl.fl}$/Tyr-NRas^{Q61K}* mice. These genetically altered cells were highly pigmented and showed a dendritic morphology, characteristic of melanocytes (Figure 3a). To test the influence of reducing activity of the MAPK/ERK pathway, we treated *Tyr-Cre Apc$^{fl.fl}$/Tyr-NRas^{Q61K}* mouse melanocytes *in vitro* with the allosteric MEK inhibitor, AZD6244 (selumetinib, ARRY--142886; Yeh *et al.*, 2007). Upon MEK inhibition, proliferation was significantly reduced, as measured by a decrease in EdU incorporation and suppression of cyclin A expression (Figure 3b–d).

A massive expansion of melanocytes in the skin of *Tyr-Cre Apc$^{fl.fl}$/Tyr-NRas^{Q61K}* mice occurs predominantly within the first 2 weeks of life (Pawlikowski *et al.*, 2013). Therefore, we reasoned that treatment of such neonatal mice with a MEK inhibitor over the first 2 weeks of life could potentially decrease melanocytic proliferation and suppress features of CMN syndrome. Mice were treated three times weekly by intraperitoneal injection with AZD6244 or DMSO vehicle for 2 weeks after birth (Figure 4a). PhosphoERK staining in the liver was markedly decreased, confirming that this regimen effectively inhibited MEK–ERK signaling in the mice (Supplementary Figure S4 online). Treatment with AZD6244 greatly reduced the population of melanocytes in the skin dermis (Figure 4b) compared to vehicle and, crucially, significantly decreased numbers of melanocytes in the CNS (Figure 4c and d). Indicative of at least partial sustained benefit from drug treatment, acute post-natal treatment with AZD6244 over 2 weeks, followed by withdrawal from therapy, resulted in a significant decrease in pigmentation within the CNS 4 weeks after the end of drug treatment (Figure 5).

DISCUSSION

Here we present several lines of evidence to indicate that, in at least a subset of cases of human CMN syndrome, the phenotype is likely to be driven by concerted aberration of NRAS and Wnt signaling. First, by whole-exome sequencing we identified a number of sequence variants in genes of the Wnt signaling pathway in DNA of peripheral white blood cells. Several of these variants are to our knowledge previously unreported, and those described are detected only at extremely low frequency in published databases. All are predicted to impair the function of the encoded protein, where *in silico* prediction is possible. Given the complexity of the Wnt signaling pathway, comprising positive and negative regulators and antagonistic interactions between canonical Wnt/β-catenin signaling and the non-canonical Wnt pathway (Niehrs, 2012), it is difficult to confidently ascertain whether these variants activate or inhibit Wnt/β-catenin signaling, without extensive additional functional studies. At this time, these sequence variants are good candidates for heritable, germ-line variants that alter activity of the Wnt signaling pathway, which we postulate may have a synergistic effect in the presence of a somatic *NRAS* mutation. Second, we observed that human CMN exhibit markers of activated Wnt signaling, suggesting that the effect of activated Wnt is not only important in the congenital development of the disease but may be involved in the post-natal persistence of the nevus. Third, in a mouse model that to our knowledge is previously unreported, we showed that melanocyte-specific activated NRAS^{Q61K} and activated Wnt signaling, through inactivation of APC, cooperate to generate features of CMN syndrome, most notably a massive excess of melanocytes in the skin and infiltration of melanocytes into the leptomeninges and CNS. Finally, post-natal systemic treatment with a MEK inhibitor, an inhibitor of NRAS signaling, reversed both the cutaneous and neurological features of this mouse model.

Previous reports have described other genetically modified mice exhibiting phenotypes that partially resemble CMN syndrome. Merlino and coworkers showed that constitutive expression of Scatter factor/hepatocyte growth factor under control of the mouse metallothionein I promoter induced melanosis in the CNS and hyperpigmentation in the skin (Takayama *et al.*, 1996). Although we cannot exclude a role for Scatter factor/hepatocyte growth factor signaling in CMN syndrome, this model does not recapitulate the most common hallmark of human CMN syndrome, *NRAS* codon 61 mutation (Kinsler *et al.*, 2013b). Several groups

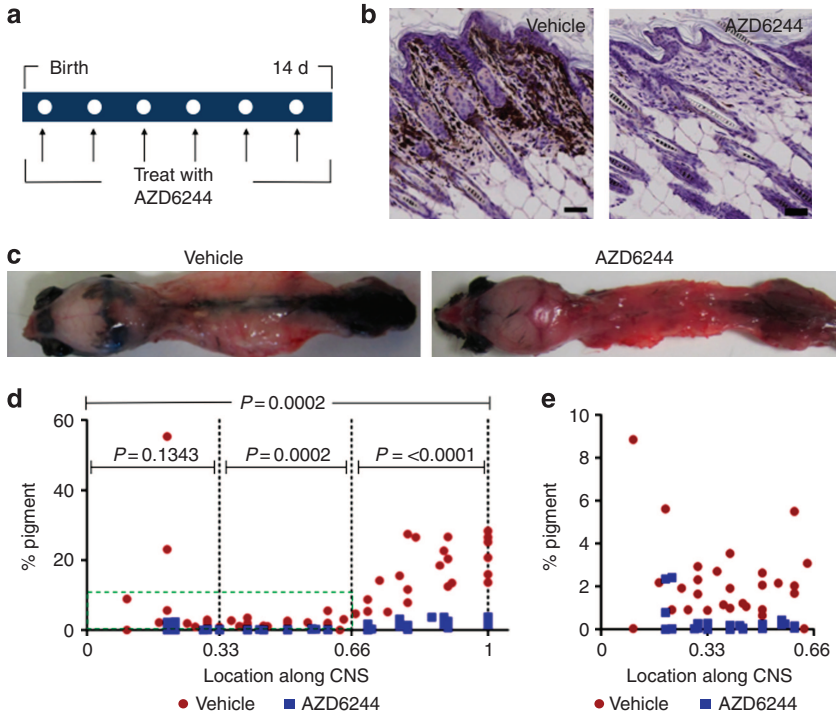

Figure 4. Inhibition of MEK suppresses features of CMN syndrome *in vivo*. (**a**) Newborn *Tyr-Cre Apc*$^{fl.fl}$*/Tyr-NRas*^{Q61K} mice were repeatedly injected IP (three times per week for 2 weeks) with vehicle or AZD6244. Two weeks later, mice were euthanized and tissues were harvested and processed. (**b**) S100 stained skin sections from *Tyr-Cre Apc*$^{fl.fl}$*/Tyr-NRas*^{Q61K} mice treated with vehicle (left) compared with AZD6244 treatment (right). **(c)** Representative images showing dorsal view of *Tyr-Cre Apc*$^{fl.fl}$*/Tyr-NRas*^{Q61K} mice treated with vehicle (left) or AZD6244 (right), after removal of the skin. (**d**) (Left) Quantitation of percent melanization in (**c**) along length of mouse from anterior of brain (0.0) to posterior of spine (1.0); (right) magnified portion of boxed region of left. Seven mice of each group with roughly ten analyses per mouse were quantitated. Linear mixed-effects model was fitted to compare the percent area between AZD6244-treated and vehicle groups. CMN, congenital melanocytic nevus; CNS, central nervous system.

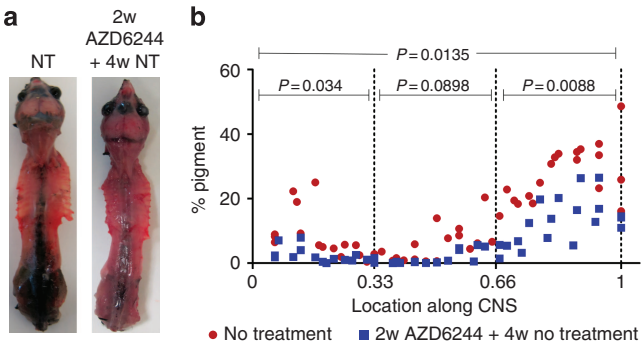

Figure 5. Acute MEK inhibition therapy has prolonged effects when given post-natally. (**a**) Representative images showing dorsal view of 6-week-old *Tyr-Cre Apc*$^{fl.fl}$*/Tyr-NRas*^{Q61K} mice either not treated (NT, left) or treated with AZD6244 for 2 weeks followed by 4 weeks off drug (right), after removal of the skin. (**b**) Quantitation of percent melanization in **a** along length of mouse from anterior of brain (0.0) to posterior of spine (1.0); analysis performed same way as Figure 4d. Three mice of each group with roughly 17 analyses per mouse were quantitated. Linear mixed-effects model was fitted to compare percent area between AZD6244-treated and -untreated groups. CNS, central nervous system.

have previously reported hyperpigmentation in the skin of mice expressing NRas^{Q61K} in the melanocyte lineage (Ackermann *et al.*, 2005; Delmas *et al.*, 2007; Shakhova *et al.*, 2012). However, consistent with our observations, none of these groups reported any neurological involvement. One of these studies found that a stabilized β-catenin allele cooperated with NRas^{Q61K} to promote melanoma (Delmas *et al.*, 2007). However, these melanomas were proposed to arise from the hair follicle bulb or the bulge region in the skin. As discussed previously (Pawlikowski *et al.*, 2013), we have not observed any frank melanoma in *Tyr-Cre Apc*$^{fl.fl}$*/Tyr-NRas*^{Q61K} mice, likely because the behavioral and neurological abnormalities associated with CNS infiltration, themselves characteristic of CMN syndrome (Barkovich *et al.*, 1994; Kinsler *et al.*, 2009; Kinsler *et al.*, 2008), preclude keeping any live mice beyond 4 months for ethical reasons.

Marais and coworkers reported in a murine model that expression of NRAS^{G12D} in the melanocyte lineage induced melanocyte proliferation and congenital melanocytic skin lesions and also primary melanoma of the CNS of variable latency but high penetrance (Pedersen *et al.*, 2013). Human CMN syndrome, however, is typically characterized by mutation of *NRAS* at codon 61, not codon 12 (Kinsler *et al.*, 2013b), although a uncommon variant of CMN is rarely associated with codon 13 mutations (Kinsler *et al.*, 2014), with a single case report of brain involvement in a patient with p.G13R (Shih *et al.*, 2014). In addition, the most common congenital CNS finding is melanosis in the parenchyma or the leptomeniges, with intracerebral primary

melanoma being a more rare and acquired phenomenon. Thus, the *Tyr-Cre Apc*$^{fl.fl}$*/Tyr-NRas*^{Q61K}mice reported here appear, to date, to be the best combined genetic and phenotypic recapitulation of human CMN syndrome.

The idea that CMN syndrome results from activated NRAS and Wnt signaling extends the model previously proposed for human acquired melanocytic nevi. Specifically, their formation is thought to depend on activated NRAS or BRAF signaling, due to oncogenic mutation of *NRAS* or *BRAF* (Omholt *et al.*, 2002; Pollock *et al.*, 2003), and also depends on input from the Wnt signaling pathway (Pawlikowski *et al.*, 2013). Normal human melanocytes are exposed to activated Wnt signaling as they migrate from the neural crest to the epidermis (Ikeya *et al.*, 1997; Dorsky *et al.*, 1998; Dunn *et al.*, 2000), and this might be the source of Wnt signaling for benign nevogenesis (Pawlikowski *et al.*, 2013), either congenital *in utero* or acquired, which typically occurs in young children (Bataille *et al.*, 2007; Zalaudek *et al.*, 2011). In some cases of CMN syndrome, we propose that somatic *NRAS* mutation cooperates with a higher level of sustained Wnt signaling resulting from germ-line genetic variants or other activators of the Wnt pathway to drive a much more severe melanocytic expansion. This germ-line modifier could provide a possible explanation for the unexplained observation of the presence or absence of neurological involvement in unrelated CMN syndrome individuals with the same cutaneous phenotype—a clinical problem that leads to all children with multiple CMN having MRI screening of the CNS in the first few months of life (Waelchli *et al.* 2015). Additional studies are required to confirm the functional significance of these variants in the pathogenesis of CMN syndrome.

Alterations of Wnt signaling in pediatric pathologies are not exclusive to CMN syndrome. For instance, more than half of all pediatric Wilms' tumor (the fourth most common childhood malignancy) have been reported to show Wnt activation (Su *et al.*, 2008). In the mouse, activation of KRAS and stabilization of β-catenin, specifically in the developing kidney, cause metastatic renal epithelial tumors to develop that mimic the epithelial component of Wilms' tumor (Clark *et al.*, 2011). As in CMN syndrome, the molecular basis of Wnt signaling activation driving this disease is often unclear (Su *et al.*, 2008). With a greater understanding of the cross-talk between *RAS* and Wnt signaling in benign and advanced disease, we may better decipher the inner workings of multiple childhood malignancies.

An understanding of the genetic basis of CMN syndrome is a likely first step to therapeutic interventions. On the basis of our previous finding that CMN syndrome is caused by somatic *NRAS* mutation (Kinsler *et al.*, 2013b), a recent report administered an oral MEK inhibitor to a 13-year-old boy with CMN syndrome in the very advanced stages of leptomeningeal melanoma (Kusters-Vandevelde *et al.*, 2014). Despite biomarker responses to the drug, the child passed away within days, as would be expected from the natural history of this malignancy at this stage. As onset of melanoma in CMN is known to require further key mutations affecting proliferative pathways (Kinsler *et al.*, 2013b), intervention before progression to malignancy is likely to be the key to success. In support of further testing of this approach, here we report that acute post-natal inhibition of MEK–ERK signaling downstream of NRAS^{Q61K} does substantially rescue the key features of CMN syndrome in this mouse model, specifically the massive expansion of melanocytes in the skin, brain, and leptomeninges. These results suggest that MEK inhibitors, currently Food and Drug Administration–approved or being trialed for use in melanoma (Sullivan and Flaherty, 2013), might also benefit patients with CMN syndrome. Importantly, although the cure of advanced melanoma through application of targeted therapies, such as MEK and BRAFV600E inhibitors (Shtivelman *et al.*, 2014), has ultimately been frustrated often by acquisition of drug resistance, conceivably this might not be a confounding factor in CMN syndrome with its many fewer genetic alterations.

MATERIALS AND METHODS

Additional details of Materials and Methods are available in Supplementary Materials and Methods online.

Human tissues

Congenital melanocytic nevi were obtained under an Institutional Review Board approved protocol by a board-certified dermatopathologist (HWM) from Fox Chase Cancer Center, Philadelphia. These tissues were fixed in 10% (vol/vol) buffered formalin for 1–3 days and embedded in paraffin, following routine histology procedure.

For whole-exome sequencing, peripheral blood leukocyte DNA was extracted from samples from 32 children with CMN attending a specialist clinic at Great Ormond St Hospital, London. Written consent was obtained in all cases, and the study was approved by the Great Ormond Street Hospital/UCL Institute of Child Health Research Ethics Committee. Detailed phenotyping of the cutaneous and neurological signs of the participants is shown in Supplementary Table S1 online, demonstrating that this group is at the severe end of the phenotypic spectrum of individuals with CMN.

Immunoblotting

Cells were lysed in 1× Laemmeli sample buffer, and 30–50 μg of protein was resolved by SDS-polyacrylamide gel electrophoresis followed by transfer onto PVDF membrane and probing with antibodies. Antibodies used include the following: anti-cyclin A (SC-754, Santa Cruz Biotechnology, Dallas, TX), anti-β-actin (A1978, Sigma, St. Louis, MO), p44/42 MAPK (Erk1/2, 4695, Cell Signaling, Danvers, MA) and phospho-p44/42 MAPK (Erk1/2, Thr202/Tyr204, 9101, Cell Signaling), anti-rabbit IgG, horseradish peroxidase-linked (NA934, GE Healthcare, Fairfield, CT), and anti-mouse IgG, horseradish peroxidase-linked (P0447, Dako, Carpinteria, CA).

Cell proliferation assays, immunofluorescence

The Click-iT EdU Alexa Fluor 594 Imaging Kit (C10339, Life Technologies, Carlsbad, CA) was used according to the manufacturer's instructions to monitor cellular proliferation.

Immunohistochemistry

Briefly, formalin fixed, paraffin embedded sections were deparaffinised, rehydrated, blocked for endogenous peroxidases, and underwent antigen retrieval according to antibody specifications. Tissues

were incubated overnight with the following primary antibodies: Anti-human melan-a clone A103 (Dako, M7196), S100 (Dako, Z0311), β-catenin (610154, BD Transduction Laboratories, San Jose, CA), CyclinD1 clone EP12 (Dako, M3642), c-myc clone 9E10 (Santa Cruz Biotechnology, sc-40), p44/42 MAPK (Erk1/2; Cell Signaling, 4695) and phospho-p44/42 MAPK (Erk1/2, Thr202/Tyr204, Cell Signaling, 9101), mouse IgG (I-2000, Vector, Burlingame, CA), and rabbit IgG (Vector, I-1000). Secondary antibodies used for DAB-based IHC were either EnVision+ System- horseradish peroxidase Labeled Polymer Anti-mouse (Dako, K4001) or EnVision+ System-horseradish peroxidase Labeled Polymer Anti-rabbit (Dako, K4003) based on primary antibody host species. Peroxidase activity was revealed using DAB (Dako, K3468). Samples were then counter-stained with haematoxylin, dehydrated, and coverslipped.

Genetically modified mice

Tyr-NRas^{Q61K} mice and *Apc*$^{fl.fl}$ mice were mated to *Tyr-Cre* mice (Shibata *et al.*, 1997; Delmas *et al.*, 2003; Ackermann *et al.*, 2005). Progenies from these crosses were then interbred to obtain *Tyr-Cre Apc*$^{fl.fl}$*/Tyr-NRas*^{Q61K} and were maintained on a C57BL6 background. Mice were kept in conventional animal facilities, monitored frequently, and experiments were carried out in compliance with UK Home Office guidelines at the Beatson Institute for Cancer Research mouse facility (Home Office PCD 60/2,607) under project license 60/4,079. Mice were genotyped by Transnetyx. Mice were first treated at their day of birth or at 1 day of age with AZD6244 (10 mg kg^{-1}) or DMSO vehicle via intraperitoneal injection and then three times per week for 2 weeks. Mice were euthanized following a Schedule 1 method, and tissues were collected for histological analyses.

Whole-exome sequencing

Whole-exome sequencing was performed in two batches of 23 and 10 samples. For the first batch, a total of 3 μg of DNA was used to prepare a DNA library using Covaris DNA sonication and NEB NEBNext DNA Sample Prep Reagent Set 1 (E6000S, New England Biolabs, Ipswich, MA). DNA fragments containing adaptors were enriched by PCR (four cycles). Samples were processed using SureSelect target Enrichment System for Illumina Paired-End Sequencing Library (Protocol version 2.0.1 May 2010). Purified libraries were checked for quality throughout the process and quantified using an Agilent (Santa Clara, CA) 2,100 Bioanalyser. Samples were sequenced using Illumina (San Diego, CA) Solexa chemistry on a Genome Analyzer IIx. Illumina 76 bp paired end kits were used according to the manufacturer's protocol. For the second batch, paired-end library preparation was by Illumina Nextera Rapid Capture Enrichment (protocol June 2013) using 50 ng DNA and sequenced on an Illumina HiSeq 2,000. Sequences were analyzed as described in Supplementary Materials and Methods online.

CONFLICT OF INTEREST

The authors state no conflict of interest.

ACKNOWLEDGMENTS

We thank Lionel Larue, Friedrich Beermann, Tetsuo Noda, and Owen Sansom for mice and advice. Thanks to all members of the PDA and VAK labs for critical discussions. This work in the laboratory of PDA was funded by CRUK Program C10652/A16566. JSP is now supported by T32HL007751, NIH Training Grant in Mechanisms of Vascular Disease. VAK was funded by the Caring Matters Now charity and supported by the National Institute for Health Research Biomedical Research Centre at Great Ormond Street Hospital for Children NHS Foundation Trust and University College London. Work carried out in the laboratory of AR was funded by NCI-RO1-CA116021 and a VA Senior Research Career Scientist award.

Author Contributions

JSP, majority of experiments and manuscript preparation. S-CC, statistical analysis. VAK, patient phenotyping and recruitment, sample collection, and exome sequencing analysis. LA-O, Sanger DNA sequencing. SP, immunohistochemistry on brain sections. EC, library prep for exome sequencing. CB, CN, FM, WL, WMH, and JMM, technical assistance. AK and KB, mouse pathology and advice. HW, human tissue and human dermatopathology. PDA, VK, and AR, supervision and manuscript preparation.

SUPPLEMENTARY MATERIAL

Supplementary material is linked to the online version of the paper at http://www.nature.com/jid

REFERENCES

Ackermann J, Frutschi M, Kaloulis K *et al.* (2005) Metastasizing melanoma formation caused by expression of activated N-RasQ61K on an INK4a-deficient background. *Cancer Res* 65:4005–11

Barkovich AJ, Frieden IJ, Williams ML (1994) MR of neurocutaneous melanosis. *AJNR Am J Neuroradiol* 15:859–67

Bataille V, Kato BS, Falchi M *et al.* (2007) Nevus size and number are associated with telomere length and represent potential markers of a decreased senescence *in vivo*. *Cancer Epidemiol Biomarkers Prev* 16: 1499–502

Bergman R, Lurie M, Kerner H *et al.* (1997) Mode of c-myc protein expression in Spitz nevi, common melanocytic nevi and malignant melanomas. *J Cutan Pathol* 24:219–22

Clark PE, Polosukhina D, Love H *et al.* (2011) beta-Catenin and K-RAS synergize to form primitive renal epithelial tumors with features of epithelial Wilms' tumors. *Am J Pathol* 179:3045–55

Danarti R, Konig A, Happle R (2003) Large congenital melanocytic nevi may reflect paradominant inheritance implying allelic loss. *Eur J Dermatol* 13: 430–2

deWijn RS, Zaal LH, Hennekam RC *et al.* (2010) Familial clustering of giant congenital melanocytic nevi. *J Plast Reconstr Aesthet Surg* 63:906–13

Delmas V, Beermann F, Martinozzi S *et al.* (2007) Beta-catenin induces immortalization of melanocytes by suppressing p16INK4a expression and cooperates with N-Ras in melanoma development. *Genes Dev* 21: 2923–35

Delmas V, Martinozzi S, Bourgeois Y *et al.* (2003) Cre-mediated recombination in the skin melanocyte lineage. *Genesis* 36:73–80

Dorsky RI, Moon RT, Raible DW (1998) Control of neural crest cell fate by the Wnt signalling pathway. *Nature* 396:370–3

Dunn KJ, Williams BO, Li Y *et al.* (2000) Neural crest-directed gene transfer demonstrates Wnt1 role in melanocyte expansion and differentiation during mouse development. *Proc Natl Acad Sci USA* 97:10050–5

Gray-Schopfer VC, Cheong SC, Chong H *et al.* (2006) Cellular senescence in naevi and immortalisation in melanoma: a role for p16? *Br J Cancer* 95: 496–505

Ikeya M, Lee SM, Johnson JE *et al.* (1997) Wnt signalling required for expansion of neural crest and CNS progenitors. *Nature* 389:966–70

Juan J, Muraguchi T, Iezza G *et al.* (2014) Diminished WNT ->beta-catenin ->c-MYC signaling is a barrier for malignant progression of BRAFV600E-induced lung tumors. *Genes Dev* 28:561–75

King R, Googe PB, Weilbaecher KN *et al.* (2001) Microphthalmia transcription factor expression in cutaneous benign, malignant melanocytic, and nonmelanocytic tumors. *Am J Surg Pathol* 25:51–7

Kinsler V, Shaw AC, Merks JH *et al.* (2012) The face in congenital melanocytic nevus syndrome. *Am J Med Genet A* 158A:1014–9

Kinsler VA, Anderson G, Latimer B *et al.* (2013a) Immunohistochemical and ultrastructural features of congenital melanocytic naevus cells support a stem-cell phenotype. *Br J Dermatol* 169:374–83

Kinsler VA, Birley J, Atherton DJ (2009) Great Ormond Street Hospital for Children Registry for congenital melanocytic naevi: prospective study 1988-2007. Part 1-epidemiology, phenotype and outcomes. *Br J Dermatol* 160:143–50

Kinsler VA, Chong WK, Aylett SE *et al.* (2008) Complications of congenital melanocytic naevi in children: analysis of 16 years' experience and clinical practice. *Br J Dermatol* 159:907–14

Kinsler VA, Krengel S, Riviere JB *et al.* (2014) Next generation sequencing of nevus spilus-type congenital melanocytic nevus: exquisite genotype-phenotype correlation in mosaic RASopathies. *J Invest Dermatol* 134: 2658–60

Kinsler VA, Thomas AC, Ishida M *et al.* (2013b) Multiple congenital melanocytic nevi and neurocutaneous melanosis are caused by postzygotic mutations in codon 61 of NRAS. *J Invest Dermatol* 133: 2229–36

Krengel S, Hauschild A, Schafer T (2006) Melanoma risk in congenital melanocytic naevi: a systematic review. *Br J Dermatol* 155:1–8

Kusters-Vandevelde HV, Willemsen AE, Groenen PJ *et al.* (2014) Experimental treatment of NRAS-mutated neurocutaneous melanocytosis with MEK162, a MEK-inhibitor. *Acta Neuropathol Commun* 2:41

Michaloglou C, Vredeveld LC, Soengas MS *et al.* (2005) BRAFE600-associated senescence-like cell cycle arrest of human naevi. *Nature* 436: 720–4

Niehrs C (2012) The complex world of WNT receptor signalling. *Nat Rev Mol Cell Biol* 13:767–79

Omholt K, Karsberg S, Platz A *et al.* (2002) Screening of N-ras codon 61 mutations in paired primary and metastatic cutaneous melanomas: mutations occur early and persist throughout tumor progression. *Clin Cancer Res* 8:3468–74

Pawlikowski JS, McBryan T, van Tuyn J *et al.* (2013) Wnt signaling potentiates nevogenesis. *Proc Natl Acad Sci USA* 110:16009–14

Pedersen M, Kusters-Vandevelde HV, Viros A *et al.* (2013) Primary melanoma of the CNS in children is driven by congenital expression of oncogenic NRAS in melanocytes. *Cancer Discov* 3:458–69

Pollock PM, Harper UL, Hansen KS *et al.* (2003) High frequency of BRAF mutations in nevi. *Nat Genet* 33:19–20

Ramirez JA, Guitart J, Rao MS *et al.* (2005) Cyclin D1 expression in melanocytic lesions of the skin. *Ann Diagn Pathol* 9:185–8

Rhodes RE, Friedman HS, Hatten HP Jr. *et al.* (1991) Contrast-enhanced MR imaging of neurocutaneous melanosis. *AJNR Am J Neuroradiol* 12: 380–2

Salama R, Sadaie M, Hoare M *et al.* (2014) Cellular senescence and its effector programs. *Genes Dev* 28:99–114

Shakhova O, Zingg D, Schaefer SM *et al.* (2012) Sox10 promotes the formation and maintenance of giant congenital naevi and melanoma. *Nat Cell Biol* 14:882–90

Shibata H, Toyama K, Shioya H *et al.* (1997) Rapid colorectal adenoma formation initiated by conditional targeting of the *Apc* gene. *Science* 278: 120–3

Shih F, Yip S, McDonald PJ *et al.* (2014) Oncogenic codon 13 NRAS mutation in a primary mesenchymal brain neoplasm and nevus of a child with neurocutaneous melanosis. *Acta Neuropathol Commun* 2:140

Shtivelman E, Davies MQ, Hwu P *et al.* (2014) Pathways and therapeutic targets in melanoma. *Oncotarget* 5:1701–52

Su MC, Huang WC, Lien HC (2008) Beta-catenin expression and mutation in adult and pediatric Wilms' tumors. *APMIS* 116:771–8

Sullivan RJ, Flaherty K (2013) MAP kinase signaling and inhibition in melanoma. *Oncogene* 32:2373–9

Suram A, Kaplunov J, Patel PL *et al.* (2012) Oncogene-induced telomere dysfunction enforces cellular senescence in human cancer precursor lesions. *EMBO J* 31:2839–51

Takayama H, La Rochelle WJ, Anver M *et al.* (1996) Scatter factor/hepatocyte growth factor as a regulator of skeletal muscle and neural crest development. *Proc Natl Acad Sci USA* 93:5866–71

Waelchli R, Aylett S, Atherton DJ *et al.* (2015) Classification of neurological abnormalities in children with congenital melanocytic naevus syndrome identifies MRI as the best predictor of clinical outcome. *Br J Dermatol* (in press)

Ye X, Zerlanko B, Kennedy A *et al.* (2007) Downregulation of Wnt signaling is a trigger for formation of facultative heterochromatin and onset of cell senescence in primary human cells. *Mol Cell* 27:183–96

Yeh TC, Marsh V, Bernat BA *et al.* (2007) Biological characterization of ARRY-142886 (AZD6244), a potent, highly selective mitogen-activated protein kinase kinase 1/2 inhibitor. *Clin Cancer Res* 13:1576–83

Zalaudek I, Schmid K, Marghoob AA *et al.* (2011) Frequency of dermoscopic nevus subtypes by age and body site: a cross-sectional study. *Arch Dermatol* 147:663–70